PROCEEDINGS OF SCIENCE

Tritium imaging with a CMOS active pixel detector

Antonio Bulgheroni [a], **Massimo Caccia** [*b], **Chiara Cappellini** [b], **Valery Chmill** [b], **Marcin Jastrzab** [bc], **Fabio Risigo**[† b]

[a] *Physics Department, University of Roma3 and INFN Roma3, via della Vasca Navale 84, Roma 00146, Italy*

[b] *Physics and Mathematics Department, University of Insubria, via Valleggio 11, Como 22100, Italy*

[c] *Electronics Department, AGH-University of Science and Technology, Al. Mickiewicza 30, Krakow 30-059, Poland*

E-mail: antonio.bulgheroni@roma3.infn.it, massimo.caccia@uninsubria.it, chiara.cappellini@uninsubria.it, chmill@particle.kth.se, jastrzab@uci.agh.edu.pl, fabio.risigo@uninsubria.it

Beta autoradiography is a well established technique to measure the distribution of macromolecules of biological interest. The potential of position sensitive solid state detectors for imaging radiolabelled samples has been widely investigated. Results on the operation of the MIMOSA5 monolithic active pixel sensor are reported in this paper, with a focus on the stability of the system and the reduction of noise generated hits.

The 16th International Workshop on Vertex detectors
September 23-28 2007
Lake Placid, NY, USA

[*]Corresponding Author and Principal Investigator.

[†]Speaker.

PoS(Vertex 2007)043

Contents

1. Introduction

Radioactive labelling is a widely used tracking method to follow the distribution of bioactive molecules throughout biological samples, in order to localize specific cell populations, proteins and, in general, molecules of biological interest [1]. In the standard panel of radiolabels (^{3}H, ^{14}C, ^{35}S, ^{32}P and ^{125}I) tritium is the most used since it can be easily bound to organic molecules, being chemically equivalent to hydrogen; moreover, the soft energy spectrum maximises the image quality. However, for the same reason, efficient detection is a real challenge. Tritium labelled biological samples are usually imaged with films and phosfor imaging plates [4], cost effective but limited by their sensitivity.

Films are disposable and cost effective ($\approx$ 100 euro/sheet), feature a very high granularity ($\approx$ few μm) and a dynamic range covering a few orders of magnitude ($\approx$ 5). Phosphor imaging plates have a sensitivity $\approx$ 100 times higher than films, are reusable and offer a dynamic range of $\approx$ 5 orders of magnitude. However both devices present undesirable features: films suffer from poor detection efficiency and phosphor imaging plates have a low image resolution, in terms of spatial resolution. The potential of silicon pixel detectors for imaging radiolabelled samples has already been demonstrated [2, 3, 4, 5, 6]. A direct comparison between two general purpose sensors, MIMOSA5 and MEDIPIX2 [5, 7], characterized by complementary technologies and architectures was performed and already reported [8]. The results do confirm the advantage of real time granular sensors against films and phosphor imaging screens, in terms of *dark counting rate* and *effective activity*. The dark counting rate is made out of two components:

- a stochastic term, related to the electronics noise and to the cosmic ray flux;
- a non-stochastic component related to either pixels featuring an extremely high leakage current or an unstable behavior and to events with an abnormal occupancy, possibly due to bias supply instabilities or pickup signals.

Table 1: Main characteristics of the MIMOSA5 sensor.

Technology	Monolithic
Array size	1024 x 1024 pixels
Redout frequency	10 MHz
Exposure time/frame	25 ms
Active Volume	0.015 mm thin, undepleted
Architecture	Full Analog, 3 transistor/cell
Output channels	4
Granularity	17 μm
Active Area	$\approx$ cm scale

The effective activity (strongly related to the sensitivity to low energy electrons) measures the ^{3}H event density rate per unit of specific activity.
In the following, the results obtained imaging tritium standards with the MIMOSA5 sensor will be presented, together with a dedicated procedure to evaluate the reduction in the dark counting rate resulting from the sensor cooling. Basic figures related to ^{3}H imaging have been measured using the RPA506 and RPA507 tritium standards. They are produced by Amersham [1] and consist of two columns of 8 active dots of 4 mm^2 area and specific activities ranging from 0.1 $\frac{nCi}{mg}$ to 109 $\frac{nCi}{mg}$. The first images of a mouse brain are also included.

2. System stabilization and basic operation procedure

The MIMOSA5 is a high granularity monolithic CMOS active pixel detector with full analog output. The device was operated untriggered and the frames were taken with a certain constant frame rate of 25 ms/frame. Its main characteristics are summarized in Table 1 and in ref. [5].

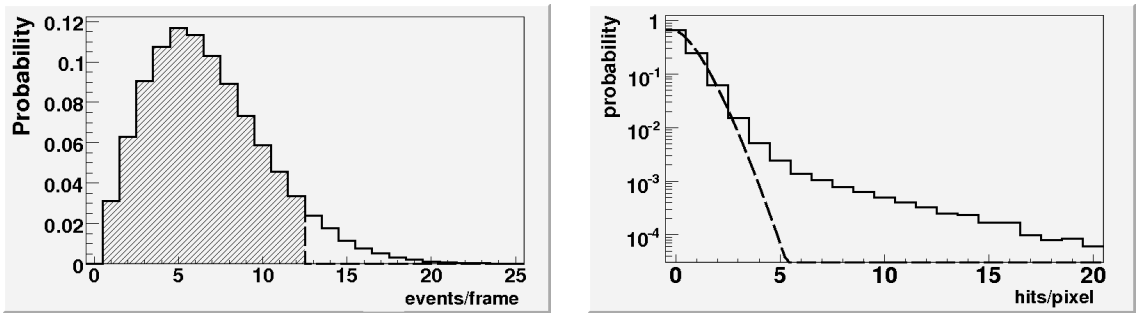

(a) **(b)**

Figure 1: *Distribution of the number of events per frame (a) and the number of hits per pixel (b). The shaded area in (a) represents the accepted frames; the dashed line in (b) represents the Poisson fit.*

[1] http://www.amersham.com/

Its sensitivity to tritium was made possible by back illuminating the sensor thinned down to 15 μm, i.e. to the thickness of the epitaxial layer [9], with a residual entrance layer of $\approx 100nm$. After this process, the MIMOSA5 is expected to have a high detection efficiency for beta rays in the keV energy range of tritium decay, featuring an equivalent noise charge (ENC) of $\approx 35\ e^-$ r.m.s. at room temperature [10, 11, 12], to be compared to a most probable value from a ^{3}H decay of 1000 e^-, distributed over a cluster with a core of 3x3 pixels [13].
The sensor was operated in a thermally controlled box, engineered to guarantee a temperature range between - 20 °C and + 35 °C with a precision of $\pm$ 0.1 °C. Because of the extremely low activities of the ^{3}H standards (from 0.1 $\frac{nCi}{mg}$ to 109 $\frac{nCi}{mg}$), the number of expected decays within an exposure time of 25 ms/frame is quite low and images result from the information contained in typically 10^5 to 10^6 frames. As a consequence, sparsification at the earliest possible step in the data acquisition chain is of utmost importance, for the optimization of both the mass data storage and the frame rate. In order not to affect the efficiency, a loose selection has been applied in real time on the cluster seed candidates, tagged and saved together with the nearest 24 neighbours. The off-line data analysis is based on two steps addressing both the non stochastic and the stochastic components of the background hits:

- **Non stochastic component:** a recursive rejection of both the entire frames recording a number of events in excess of a parametrized cut and of the single pixels presenting a dysfunctional behaviour has been developed. The method is described in Figure 1: a frame is rejected if it contains a number of clusters 2 σ away from the most probable value of the events per frame distribution (Figure 1(a)). Moreover, a pixel is masked if its behaviour differs from what can be expected by a Poissonian distributed pixel occupancy (Figure 1(b)).

- **Stochastic component:** a preliminary cut of 5.75 σ on the signal over noise ratio of the seed has been applied; this choice has been performed in order to maximise the background hit rejection, relying on the plots shown in Figure 2. In addition a bayesian discrimination algorithm against the hypothesis that each cluster is noise generated has then been applied. It has been developed following the method described in [14] and it is summarized in [8].

An analysis of the the noise spectra recorded at different temperatures was also performed and the results are shown in Figure 3. The most probable value of the noise decreases by $\approx$ 10% going from room temperature to 4 °C. Whether numerically small, this effect does have an impact on the effective activity where the variation is amplified by a factor corresponding to the selection threshold (see Table 2 and Table 3). The asymmetry of the spectrum at high noise values is mostly related to spatial inhomogeneites of the sensor. At 4 °C the effect is highly suppressed. Moreover, a subset of pixels features a value dominated by the system noise, measurable without the sensor connection and peaking at $\approx$ 1.5 ADC. The overall effect of the stabilization and cooling may be quantified applying the selection criteria described above for the non stochastic noise: the number of rejected frames decreases from $\approx$ 10% at room temperature to $\approx$ 3% at 4 °C, while the number of masked pixels decreases from $\approx$ 2.5% to $\approx$ 1%. The spread among different quarters in the

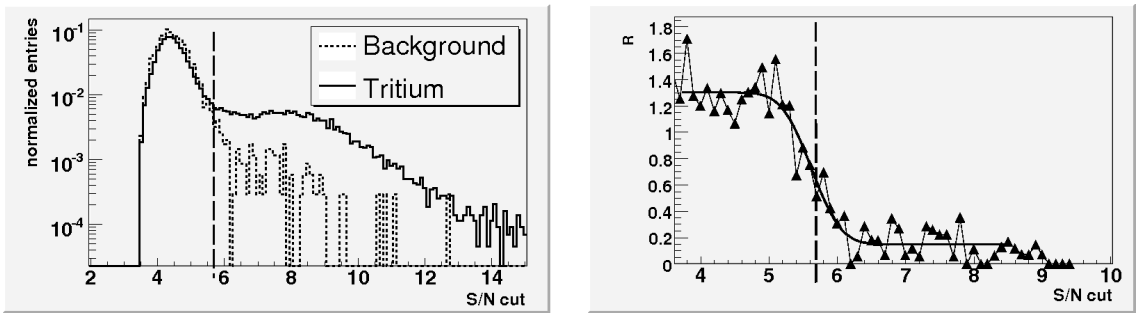

(a) **(b)**

Figure 2: *Signal over noise spectra of the seed pixel for an empty and a tritium run and relative ratio. The plots are normalized to the total number of entries. R is the value of the bin-to-bin ratio in the spectra shown in (a). The dashed line represents the preliminary cut of 5.75 σ on the signal over noise ratio of the seed.*

number of rejected frames and masked pixels is also decreasing from $\approx 7\%$ to $\approx 0.01\%$ and from $\approx 3.6\%$ to $\approx 0.85\%$, thus resulting in a net improvement of the sensor uniformity.

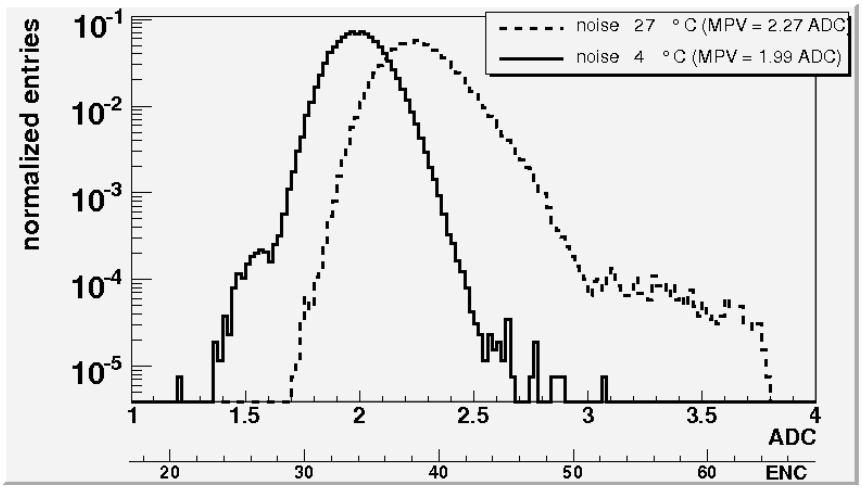

Figure 3: *The noise spectra recorded at different temperatures. The plots are normalized to the total number of entries.*

3. Biological sample Imaging

The sensor sensitivity to ^{3}H was measured relaxing on the RPA 506 and RPA 507 standards. An image is show in Figure 4. The effective activity and sensitivity at room temperature and 4 °C are reported in Table 3. The sensor sensitivity corresponds to the specific activity in $\frac{nCi}{mg}$ resulting in a count density rate equals to 3 times the fluctuations of the background.
Commercially available phosphor imaging plates claim a minimum detectable density rate of 30 $\frac{dpm}{mm^2}$ for ^{14}C for the BAS Fuji film. This represents the minimum density rate the system is able to detect. The characterized pixel sensor has featured a minimum value of $\approx 10^{-2} \frac{dpm}{mm^2}$.

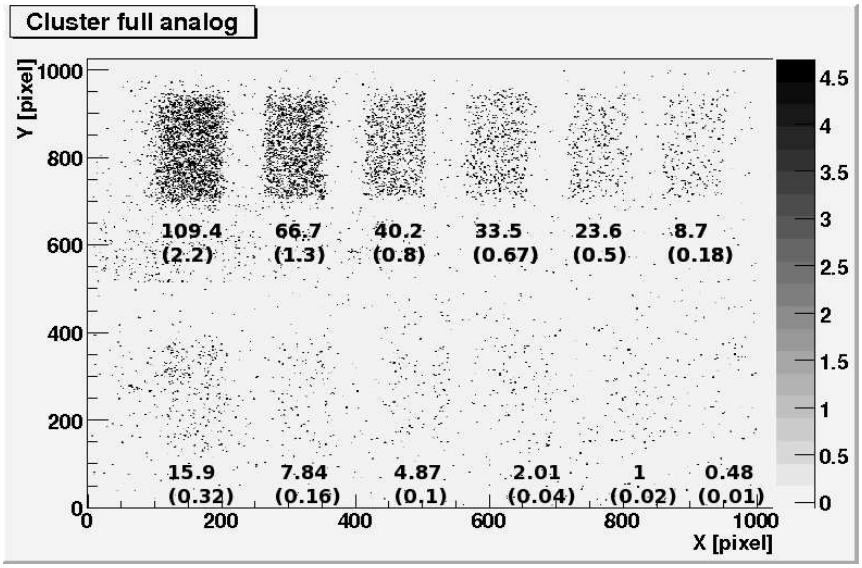

Figure 4: *Imaged recorded at 4 °C. Activities are expressed in* $\frac{nCi}{mg}$ *(kBq).*

Table 2: Background hit density rate at room temperature and at 4 °C

	room temperature $[\frac{counts}{mm^2 \cdot s}]$	4 °C $[\frac{counts}{mm^2 \cdot s}]$
Raw data	4.7 ± 0.013	$(9.0 \pm 0.03) \cdot 10^{-1}$
Before stochastic rejection	$(7.5 \pm 0.16) \cdot 10^{-2}$	$(3.3 \pm 0.17) \cdot 10^{-3}$
After stochastic rejection	$(2.6 \pm 0.16) \cdot 10^{-2}$	$(6.6 \pm 0.78) \cdot 10^{-4}$

Table 3: Effective Activity (EA) and sensor sensitivity at room temperature and at 4 °C

		room temperature	4 °C
EA $[\frac{counts}{mm^2 \cdot s \cdot \frac{nC}{mg}}]$	Raw data	$(3.7 \pm 0.03) \cdot 10^{-2}$	$6.3 \cdot 10^{-3} \pm 1.52 \cdot 10^{-4}$
	Before stochastic rejection	$(1.41 \pm 0.073) \cdot 10^{-3}$	$1.3 \cdot 10^{-3} \pm 3 \cdot 10^{-5}$
	After stochastic rejection	$(5.7 \pm 0.47) \cdot 10^{-4}$	$7.5 \cdot 10^{-4} \pm 2.3 \cdot 10^{-5}$
	Sensor sensitivity $[\frac{dpm}{mm^2}]$	$\approx 3 \cdot 10^{-1}$	$\approx 1.4 \cdot 10^{-2}$

The impressive sensitivity of the pixel system is made clear by the first series of recorded pictures of real biological samples, namely slices of a mouse brain. As exemplary illustration, the same sample imaged with a film over a week and using the mimosa over a run of 10 hours (effective exposure time) with the respective slices are shown in Figure 5. The slices show a direct comparison between the film and the MIMOSA sensor in terms of image contrast.

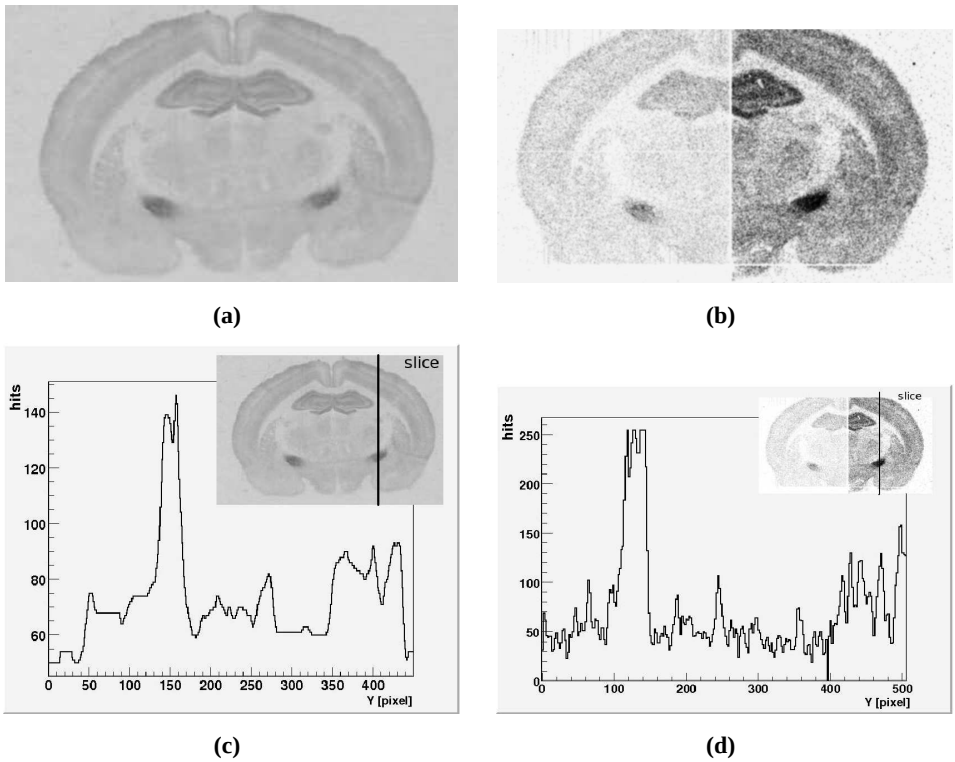

Figure 5: *Tritium labelled slice of mouse brain recorded with a film over a week at room temperature (a) and with MIMOSA5 over a run of 10 hours (effective exposure time) at 4 °C (b). In Figure (b) the difference between the two columns is due to the difference in the diode dimension. In the left column the diode is 9.6 pm^2; in the right one it is 24 pm^2. In Figure (c) and (d) a slice of mouse brain is presented.*

4. Conclusion

The reported results assess the enormous potential of silicon pixel detectors in radiolabelled sample imaging. The MIMOSA5 pixel sensor has featured a sensitivity of $\approx 10^{-2} \frac{dpm}{mm^2}$ for ^{3}H to be compared to 30 $\frac{dpm}{mm^2}$ on ^{14}C for the BAS Fuji film.

At the moment, the development of a dedicated instrument is severely constrained by the required area and the related complexity in real-time data handling: in fact, the typical biological investigation requires a simultaneous imaging of 20 - 40 samples, each of which would be possible with a single mimosa-like sensor.

However, advances in the development of detectors with on-cell architectures for real time sparsification are quite rapid and, on a mid-term, could make the exploitation of this technique possible.

References

[1] T. Nagata, *Progress in Histochemistry and Cytochemistry* **37**, 59 (2002).

[2] J. Ulrici *et al.*, *Nucl. Instrum. Meth. A* **465**, 247 (2001).

[3] J. Ulrici *et al.*, *Nucl. Instrum. Meth. A* **547**, 424 (2005).

[4] J. Cabello, *Physics in medicine & biology* **52**, 4993 (August 2007).

[5] G. Deptuch *et al.*, *Nucl. Instrum. Meth. A* **A511**, 240 (2003).

[6] G. Mettivier, M. C. Montesi and P. Russo, *Nucl. Instrum. Meth. A* **516**, 554 (2004).

[7] Medipix collaboration web site (http://www.cern.ch/medipix).

[8] C. Cappellini, A. Bulgheroni, M. Caccia, V. Chmill, M. Jastrzab, F. Risigo and E. Scopelliti, *to be published in Nucl. Instrum. Meth. A* (2007).

[9] W. Dulinski, A. Braem, M. Caccia, G. Claus, G. Deptuch, D. Grandjean, C. Joram, J. Séguinot and M. Winter, *Nucl. Instrum. Meth. A* **546**, 274 (2005).

[10] G. Deptuch, *Nucl. Instrum. Meth. A* **543**, 537 (2005).

[11] R. Turchetta, J. D. Brest, B. Casadei, G. Claus, C. Colledani, W. Dulinski, Y. Hu, D. Husson, J. P. Le Normand, J. L. Riester, G. Deptuch, U. Goerlach, S. Higueret and M. Winter, *Nucl. Instrum. Meth. A* **458**, 677 (2001).

[12] Y. Gornushkin *et al.*, *Nucl. Instrum. Meth. A* **A478**, 311 (2002).

[13] Y. Gornushkin *et al.*, *Nucl. Instrum. Meth. A* **A513**, 291 (2003).

[14] G. Borisov and C. Mariotti, *Nucl. Instrum. Meth. A* **A372**, 181 (1996).